

RSC Advances



This is an *Accepted Manuscript*, which has been through the Royal Society of Chemistry peer review process and has been accepted for publication.

Accepted Manuscripts are published online shortly after acceptance, before technical editing, formatting and proof reading. Using this free service, authors can make their results available to the community, in citable form, before we publish the edited article. This *Accepted Manuscript* will be replaced by the edited, formatted and paginated article as soon as this is available.

You can find more information about *Accepted Manuscripts* in the [Information for Authors](#).

Please note that technical editing may introduce minor changes to the text and/or graphics, which may alter content. The journal's standard [Terms & Conditions](#) and the [Ethical guidelines](#) still apply. In no event shall the Royal Society of Chemistry be held responsible for any errors or omissions in this *Accepted Manuscript* or any consequences arising from the use of any information it contains.

that porous silicon nanoparticles coated by leukocyte membrane could effectively prolonged the *in vivo* circulation time, avoided clearance by immune system and increased nanoparticles accumulation in tumor sites.¹²

SPIO has been approved as a clinical MRI contrast agent. In addition to its molecular imaging application, under a high-frequency AMF, SPIO can rapidly change its magnetic moment where the friction produces heat for hyperthermia therapy applications.¹³ Surface modifications are often required to afford SPIO with long circulating ability for better theranostic efficacy.¹⁴ In this study, we proposed using low immunogenic stem cell membrane as a novel surface modification material to prepare biomimetic membrane-camouflaged SPIO. Mesenchymal stem cell (MSC) is a class of multipotent cells, which are capable of differentiating into various cell lineages such as osteoblast, chondrocyte, adipocyte and myoblast.¹⁵ In addition, MSC is low immunogenic and exhibits immunomodulatory activity *in vivo*.^{16,17} As a potential source of cell membranes, MSCs can be harvested from various tissues and expended in large quantity *in vitro*. So far, using stem cell membrane (STM) for the surface modifications of functional nanoparticles has not been reported yet.

In this study, the STM-camouflaged SPIO was prepared by utilizing simple sonication method. The prepared STM-SPIO was characterized for the particle size. STM coating on SPIO was tested using TEM, fluorescence dye retention assay, total membrane protein analysis and antibody binding assay. The magnetic properties of STM-SPIO were examined using superconducting quantum interference device (SQUID) and T2 MRI imaging. The effects of STM coating on the prevention of macrophage uptake were examined by Persian Blue Staining and ICP-MS methods. The magnetic hyperthermia properties of STM-SPIO was measured and applied for cancer cell treatment.

2. Experimental

2.1 Materials.

Magnesium chloride, sucrose, sodium phosphate dibasic, sodium phosphate monobasic, citric acid, Coomassie Brilliant Blue R250 and ammonium hydroxide were purchased from Sigma-Aldrich (St. Louis, MO, USA). Tris-base and MTT were purchased from MDBio, Inc. (Taipei, Taiwan). Fluorescein Isothiocyanate (FITC)-anti-CD44 antibody (103006) and PE-Rat IgG2b/ κ Isotype Ctrl Antibody (400608) were purchased from Biolegend (San Diego, CA, USA). Anhydrous iron (II) chloride and iron (III) chloride were purchased from Alfa Aesar (Ward Hill, MA, USA). Collagenase I was purchased from Worthington (Freehold, NJ, USA). Dulbecco's Modified Eagles Medium (DMEM) and Minimum Essential Medium- α (α -MEM) were purchased from Gibco (Carlsbad, CA, USA). Penicillin-streptomycin (P/S) and fetal bovine serum (FBS) were purchased from Hyclone (Logan, UT, USA).

2.1 Synthesis of citric acid-capped SPIO (CA-SPIO).

The citrate-coated SPIO were synthesized by co-precipitation method.¹⁸ Briefly, 324.4 mg of FeCl_3 and 127 mg of FeCl_2 ($\text{Fe}^{3+}:\text{Fe}^{2+} = 2:1$ of molar ratio) were dissolved in 15 mL of DI H_2O in a three-necked flask under argon condition and heated up to 75 °C. Then 5 mL of 28% NH_4OH was added into the mixture with vigorous stirring for 30 minutes. Afterwards, 200 mg of citric acid dissolved in 2 mL DI H_2O was slowly introduced into the reactant and kept stirring at 75 °C for another 30 minutes to obtain SPIO. The as-synthesized SPIO was collected by magnetic attraction and washed with DI H_2O three times to remove NH_4OH and excess citric acid. The purified SPIO was resuspended in 10 mL DI H_2O and its iron concentration was determined by potassium thiocyanate (KSCN) methods.¹⁹

2.3 Quantitation of total iron by KSCN methods.

SPIO samples (50 μL) were mixed with 50 μL 12 N HCl and 50 μL 30% ammonium persulfate and incubated at 65 °C for 1 hour to dissociate SPIO and oxidize ferrous ions to ferric ion. After cooling down to room temperature, the mixture was mixed with 100 μL 5% KSCN and determined the absorbance at 470 nm. A series of ferric chloride diluted solutions prepared in 12N HCl were used for standard calibration.

2.4 Isolation and characterizations of adipose-derived MSCs.

The adipose-derived MSCs were obtained from C57BL/J mice.²⁰ The mice were sacrificed by CO_2 and dissected the adipose tissue from subcutaneous site of lower abdomen. The tissue was cut into pieces and washed by PBS several time till the color of PBS turning transparent before digested with 0.1 % collagenase I in PBS for 1 hour at 37 °C. During the digestion, shake the sample every 20 minutes. The released cells were centrifuged at 300 g for 5 minutes to remove the floating fat. The cell pellet was resuspended with PBS and filtered through 70 μm cell strainer (BD). The cells were collected by centrifuged at 300 g for 5 minutes and then resuspended with α MEM supplemented with 20% FBS and 1x Penicillin and streptomycin. The whole cells were sorted to collect CD44 and CD73 positive cells using FACS Aria™ III (BD).

2.5 Isolation of STM.

The STM was isolated according to a published procedure.²¹ In brief, MSCs (1×10^7 cells) were harvested, washed with PBS and resuspended in cold Tris-Magnesium buffer (TM-buffer pH= 7.4). Cells were homogenized at 22,000 rpm for 1 minute before adding TM-buffer/60% sucrose to a final concentration of 5% sucrose. The homogenized cells were collected by centrifugation at 6,000 g for 15 minutes and then washed twice with 0.15 M sucrose/TM-buffer (pH 7.4). To completely remove cell organelles and obtain smaller fragments of STM, the collected pellet fraction was subjected to further homogenization by Sonics VCX 750 W probe sonication (Sonics, Newtown, CT, USA; maximum power: 750 W; frequency: 20 kHz; probe diameter: 13 mm) at 27% amplitude of maximum power for 5 seconds and washed twice as described above. The STM was collected by centrifugation at 6,000 g for 15 minutes and resuspended in DI H₂O for STM-SPIO preparation.

2.6 STM-SPIO preparation by sonication.

To assemble the STM onto SPIO, fixed amount (1 mg) of STM was mixed with SPIO at various weight ratios (STM : SPIO = 1:1, 3:1, 5:1, 20:1) in 4 mL of 10 mM Na₂HPO₄/NaH₂PO₄ buffer. The mixture were incubated on ice for 30 minutes and then subjected to probe sonication at 27% amplitude for 40 seconds (5 seconds/5 seconds; on/off, 8 times). The as-synthesized STM-SPIO was collected by magnetic attraction, washed twice with DI H₂O and resuspended in DI H₂O for further usage.

2.7 Physicochemical characterizations of SPIO and STM-SPIO.

Particle size of the as-synthesized STM-SPIO in DI H₂O was measured using ZetaSizer Nano Series (Malvern, UK). For the colloidal stability test, STM-SPIO was added into DI H₂O, 25% FBS/DMEM or 50% FBS/DMEM for particle size measurement. The magnetism of SPIO or STM-SPIO was measured using the SQUID at 300 K (Quantum Design MPMS-XL, USA). For TEM imaging (JEOL JEM-1200EX II, Japan), the samples were prepared by dropping SPIO or STM-SPIO solution onto copper TEM grids and negatively stained with 1% tungstophosphoric acid before acquiring images.

2.8 Coverage of STM on SPIO by dye retention assay

To verify the presence of STM on SPIO, 1 μ L or 10 μ L of DiO (0.5 mg/mL in DMSO) were mixed with 1 mg of STM-SPIO or unmodified SPIO in 4 mL of 10 mM Na₂HPO₄/NaH₂PO₄ buffer then sonicated for 20 seconds (5 seconds/5 seconds; on/off). The SPIO-containing samples were collected by magnetic attraction and washed with DI H₂O twice to remove unbound DiO. The STM-SPIO or SPIO were resuspended in DI H₂O. STM-SPIO or SPIO containing 80 μ g Fe was detected for its DiO fluorescence using a fluorescence plate reader (ex: 460 nm/em: 495 nm - 600 nm).

2.9 Protein retention by SDS-PAGE.

The protein retention of STM on STM-SPIO was confirmed by SDS-PAGE. STM extracted from 7×10^6 MSCs or STM-SPIO prepared with the same amount of STM was mixed with 6x loading buffer to total volume of 70 μ L then subjected to protein denature process (heating at 85 °C for 10 minutes). The samples were analyzed on SDS-PAGE (12% polyacrylamide for protein separation). Gel was stained by Coomassie Brilliant Blue for 20 minutes and then destained in 30% methanol/10% acetic acid before acquiring gel images using an optical scanner (TX220, EPSON).

2.10 Antibody binding assay.

The further confirm the preservation of stem cell marker CD44 on STM-SPIO, the antibody binding assay was performed. 5 μ g CD44-FITC antibody was mixed with 10 μ g or 100 μ g STM-SPIO as w/w ratios (CD44-Ab : STM-SPIO) of 1:2 or 1:20 respectively. 2 μ g of isotype-PE control antibody was mixed with 100 μ g STM-SPIO and used as the negative control. The mixtures were incubated on ice for 2 hours. The STM-SPIO was collected by magnetic attraction and the supernatant which contained the unbound antibody-FITC was detected for the fluorescent intensity using a plate reader. (FITC: ex: 490 nm/em: 520 nm; PE: ex: 540 nm/em: 580 nm).

2.11 T2-weighted imaging of STM-SPIO

T2-weighted images and transverse relaxivity (R₂) of STM-SPIO were determined using a 7T MR imaging system (Bruker biospec 70/30 MRI, USA). Different ferric iron concentrations of STM-SPIO (1, 0.5, 0.25, 0.125 and 0.0625 mM Fe) in DI H₂O were transferred into 250 μ L PCR tubes for images scanning. A multislice multiecho (MSME)-T2 map pulse sequence²² with fixed TR (6000 ms) and 32 echoes in 11 ms intervals was used to measure the spin-spin relaxation times (T₂) of STM-SPIO. A T2-weighted spin-echo sequence (TR/TE = 6000 ms/11 ms) with the following parameters: TR/TE = 6000 ms/11 ms, matrix size = 256 \times 256, FOV = 6 \times 6 mm and NEX=3 was used for MR imaging.

2.12 Cell culture

TRAMP-C1 and RAW246.7 cells were cultured in DMEM supplemented with 10% FBS and 1x P/S maintained at 37 °C and 5% CO₂ atmosphere. MSCs were cultured in α -MEM supplemented with 20% FBS and 1x P/S at 37 °C and 5% CO₂ atmosphere. The cells were subcultured at split ratio of 4:1 while cells confluency reached 90%.

2.13 Macrophage uptake of STM-SPIO

1 x 10⁵ RAW246.7 cells were seeded in 24-well plates and cultured at 37 °C overnight. After the cell confluency reached 60%, the cells were rinsed with PBS and the medium was replaced with 25% FBS/DMEM. The Fe content of SPIO or STM-SPIO was determined using KSCN methods as previously described. SPIO or STM-SPIO was added to the cells at final Fe concentration of 10, 20 or 30 μ g/mL then incubated for 4 hours. After that, the cells were washed twice with PBS then fixed by 4% paraformaldehyde/PBS at room temperature for 10 minutes. To visualize the intracellular SPIO, the cells were treated with Prussian Blue Staining (10% hexacyanoferrate in 20% hydroxyl chloride solution) for 20 minutes and washed twice with DI H₂O before taking the cell images using Zeiss Axio Observer D1. (Carl Zeiss, Oberkochen, Germany). On the other hand, the cells were detached by trypsinization then subjected to fixation for determining the amount the uptake SPIO using ICP-MS. The results were normalized to the amount of total cell proteins measured by BCA assay (Pierce).

2.14 Magnetically-assisted cellular uptake of STM-SPIO

1 x 10⁵ TRAMP-C1 cells were seeded in 24-well plates and cultured at 37 °C overnight. After the cell confluency reached 60%, the cells were rinsed with PBS and the medium was replaced with 10% FBS/DMEM. STM-SPIO was added into well to final concentration of 20 μ g/mL or 150 μ g/mL then incubated for 4 hours with or without magnetic attraction. After that, the cells were washed twice with PBS and then fixed by 4% paraformaldehyde/PBS before Prussian Blue Staining as previous described.

2.15 Magnetic hyperthermia treatment

The magnetic hyperthermia effect of SPIO or STM-SPIO was first evaluated by placing SPIO or STM-SPIO solution (200 μ g/mL) under AMF treatment for 20 minutes (Power-cube 32 High Frequency Induction System, President Honor Industries Co., New Taipei City, Taiwan) with field frequency (1.024 MHz), average applied power on coil (32 kvar) and maximum absorbed power (2.8 kW). To further evaluate the effect of magnetic hyperthermia effect of STM-SPIO on TRAMP-C1 cells, 4 x 10⁵ cells were seeded in 6-well plates and cultured overnight. When the cell confluency reached 70 %, TRAMP-C1 cells were washed with PBS and the medium was replaced with fresh 10 % FBS/DMEM. STM-SPIO were added into the medium at 100 μ g/mL or 150 μ g/mL then incubated with or without magnetic attraction for 4 hours. Next, the cells were washed with PBS twice, trypsinized before resuspending in 250 μ L medium at cell concentration of 1.5 x 10⁶ cells/mL to receive AMF treatment (same parameters as above mentioned). 5, 10, 15, 20 minutes after the beginning of AMF treatment, the solution temperature was recorded using an infrared thermal camera (AVIO F30S, NEC Avio Infrared Technologies, Tokyo, Japan). After that, the cells were reseeded into 24-well plates and cultured for additional 20 hours before determining the cell viability using MTT assay.

2.16 Statistical analysis

All statistical evaluations were carried out using unpaired two-tailed Student's t-test. p-value of less than 0.05 was considered significant (p < 0.05, * ; p < 0.01, ** ; p < 0.001, ***).

3. Results and discussion

3.1 Preparation and characterizations of STM-SPIO.

Adipose-derived MSCs were collected and treated with hypotonic (0.25 X PBS) solution following by mild homogenization to break up cells into cytosol, nucleus and cell membranes. The cell membranes were washed by repeated centrifuge steps to remove nucleic acids and cytosolic components. The aforementioned procedure for STM isolation was performed on ice bath to minimize the denaturation of cell membrane-associated proteins. SPIO was synthesized by co-precipitation method. The as-synthesized SPIO was water-soluble and exhibited good superparamagnetic properties. To fabricate STM-SPIO, the STM was added into SPIO solution then subjected to a mild sonication on ice bath. Sonication provided energy to force the cell membrane physically disassemble and reassemble with the SPIO into STM-SPIO in the aqueous solution (Scheme 1). To optimize the preparation of STM-SPIO, different weight ratios of STM and SPIO (STM : SPIO = 1:1, 3:1, 5:1, 20:1) were attempted (Figure 1A). The hydrodynamic size of the prepared STM-SPIO was measured using a ZetaSizer. At all the tested weight ratios, the formed STM-SPIOs exhibited increased size compared to the SPIO. The increased size might be due to the coverage of STM on the surface of SPIO. However, further increase on STM amount contributed to the formation of large aggregated nanoparticles. Based on these results, STM : SPIO at weight ratio of 1:1 was used to fabricate nano-sized STM-SPIO for the subsequent studies. In addition, the Fe content in STM-SPIO (1:1) was 85.17% \pm 5.94% measured using KSCN methods. To visualize the presence of

membrane structure on STM-SPIO, the particles were negatively stained with tungstophosphoric acid and observed using TEM (Figure 1B). The results suggest SPIO cluster were covered with membrane structure in STM-SPIO compared to naked SPIO. STM coating on the surface of SPIO was further characterized by a dye retention assay where the hydrophobic fluorescent dioctadecyloxycarbocyanine perchlorate (DiO) was employed. DiO was mixed with SPIO or STM-SPIO in an aqueous solution then received sonication following by repeated magnetic attraction to remove the unbound DiO. The fluorescence intensity of DiO (ex: 460 nm/em: 495 - 600 nm) was detected using a fluorescence spectroscopy. As the negative control, the STM or SPIO was verified to be non-fluorescent. The results (Figure 2) show that higher fluorescence intensity was observed from STM-SPIO compared to SPIO, which can be explained by the presence of lipid bilayer structure in STM providing a hydrophobic reservoir for the hydrophobic DiO molecules. The intensity of DiO fluorescent was increased when loading higher amount of DiO to the STM-SPIO. Next, SDS-PAGE analysis was utilized to analyze the retention of STM-associated proteins on STM-SPIO. Similar overall protein profile was observed from the fresh STM and extracts of STM-SPIO (Figure 3A) suggesting that the optimized fabrication procedure did not cause significant decline of total proteins from the STM.

CD44-positive MSCs were used as the source of STM in this study. The retention of stem cell marker CD44 in the membrane structure of the prepared STM-SPIO was further characterized by using an antibody binding assay (Figure 3B). FITC-labelled anti-CD44 antibody (CD44-FITC) was incubated with STM-SPIO at the weight ratios of 1:2 or 1:20 for 2 hours then subjected to centrifuge to pull down the CD44-FITC/STM-SPIO complexes. The unbound CD44-FITC in the supernatant was measured for the fluorescence intensity using a fluorescence plate reader. The decrease of fluorescence intensity was observed from the higher binding ratio of STM-SPIO to CD44-FITC. In contrast, unchanged fluorescence was observed from the isotype control antibody/STM-SPIO binding group. The result suggests stem cell maker: CD44 was well preserved after the mild sonication procedure for STM-SPIO preparation.

3.2 Colloidal Stability of STM-SPIO

Taking advantages of its nano-size and magnetic properties, SPIO could be directed to cancer sites via passive (EPR effect) or active targeting (magnetic targeting) for potential theranostic applications on cancers. Without appropriate surface modifications, SPIO is prone to form aggregation in serum-containing conditions.²³ Poor *in vivo* colloidal stability of unmodified SPIO is responsible for its rapid clearance by the RES organs such as liver and lung thus limiting its theranostic applications. To achieve efficient drug delivery, it is crucial to develop carriers with good colloidal stability under physiological conditions. In this study, the size evolution of STM-SPIO under various conditions including DI H₂O, 25% serum and 50% serum-containing DMEM was studied using DLS techniques (Figure 4). The initial size (10 minutes incubation) of STM-SPIO was measured as: 141.1, 391.1 and 282.9 nm in DI H₂O, 25% or 50% serum respectively. These particle sizes still fall within the range for EPR effect.²⁴ After the extended incubation time (4 and 24 hours), the size of STM-SPIO in DI H₂O was not changed significantly suggesting its stable colloidal structure. Similar size evolution trend was also observed from STM-SPIO incubated under serum-containing environments. It is noticed that the size of STM-SPIO was larger in serum-containing medium compared to H₂O. This phenomenon might be attributed to the salt-mediated charge neutralization on the surface of STM-SPIO, which could promote particle aggregation. Overall, the results suggest that STM-SPIO possess good colloidal stability and is worth further evaluation for its potential *in vivo* theranostic applications.

3.3 Magnetic properties of STM-SPIO

The magnetization and hysteresis loop of STM-SPIO were examined using SQUID (Quantum Design MPMS-XL, USA). The magnetization of SPIO and STM-SPIO was measured to be 72.7 and 65.9 emu/g respectively (Figure 5A). Both samples showed typical superparamagnetic curve, and the lower magnetization of STM-SPIO might be attributed to the weight contribution of STM. To evaluate the potential of using STM-SPIO as a novel MRI contrast agent, various concentrations of SPIO or STM-SPIO were fixed in agarose phantoms and imaged by 7T MR imaging system. The transverse relaxivities (R₂) for STM-SPIO and SPIO were 653.3 and 786.0 s⁻¹mM⁻¹ respectively measured by multislice multiecho (MSME)-T₂ map pulse sequence (Figure 5B). A concentration dependent T₂-weighted MRI imaging contrast was observed from the STM-SPIO solutions (Figure 5C).

3.4 Macrophage uptake of STM-SPIO

Foreign materials such as theranostic nanoparticles, after they were injected systemically, could elicit various host defense responses including opsonization and phagocytosis by macrophages resided in the reticuloendothelial system (RES) of liver and lung. As a result, rapid clearance of nanoparticles could lead to ineffective theranostic efficacy and side effects in the normal organs. It has been previously shown that surface modifications with red blood cells- or leukocytes-derived biomembranes represent an effective approach to prepare long-circulating nanoparticles. The underlying mechanism is attributed to the presentation of marker of self on the biomembrane-camouflaged nanoparticles. For example, CD47 on red blood cell membrane could inhibit macrophage uptake via interacting with the SIRP α (signal-regulatory protein alpha) on macrophage surface.⁹ In this study, the effect of STM coating on preventing SPIO uptake by macrophages was examined. STM-SPIO or SPIO was incubated with mouse macrophage cell line (RAW 264.7), which shows active phagocytic activity. The Fe content of the added SPIO or STM-

SPIO was quantitated using KSCN methods. SPIO or STM-SPIO were added to the cells to final Fe concentrations of 10, 20 or 30 $\mu\text{g/mL}$ and incubated for 4 hours. After incubation and washing steps, the intracellular SPIO was visualized as blue spots using Prussian Blue Staining. The cell images show that (Figure 6A), within the same incubation conditions (time length and SPIO concentration), the macrophage uptake of STM-SPIO was less than SPIO. Furthermore, ICP-MS was used to accurately measure the intracellular Fe content. Macrophages incubated with SPIO or STM-SPIO were harvested and subjected to nitric acid digestion for ICP-MS analysis. The measured values of Fe for each group were 0.08 ppm (control), 16 ppm (SPIO) and 6.55 ppm (STM-SPIO) in the cell digest. After normalizing by cellular total protein amount, the results (Figure 6B) show that the intracellular Fe content was significantly higher ($p < 0.05$) for SPIO (0.02257 mg Fe/ mg protein) than STM-SPIO (0.00836 mg Fe/mg protein). Taken together, it is suggested STM coating could significantly decrease SPIO uptake by macrophages.

3.5 Magnetic hyperthermia by STM-SPIO

When SPIO is placed under an external AMF, heat will be generated from magnetic moment relaxation through Neel or Brown mechanism. By using an infrared thermal camera (Figure 7), it was observed that STM-SPIO and SPIO possessed similar magnetic induced hyperthermia effect. Next, the cellular uptake of STM-SPIO by cancer cells was examined. Mouse prostate cancer cells (Tramp-C1) were incubated with STM-SPIO (20 or 150 $\mu\text{g/mL}$) for 4 hours following by washing out the un-internalized STM-SPIO. By using Prussian Blue Staining (Figure 8), it was observed that the uptake of STM-SPIO by Tramp-C1 cells was dose-dependent. Under the attraction by an external magnet, darker blue staining was observed inside the cells indicating the enhanced intracellular internalization of STM-SPIO. The enhanced cellular uptake of STM-SPIO by an external magnetic field could be explained by the accelerated sedimentation of nanoparticles to the cell surface which in turn to promote the endocytosis.²⁵ The temperature rising effect of STM-SPIO in Tramp-C1 cells was investigated next. The cells were incubated with 2 different STM-SPIO concentrations with or without the attraction by an external magnet. The trend of temperature rising effect is summarized as the followings: 150 $\mu\text{g/mL}$ (Magnet+) > 150 $\mu\text{g/mL}$ (Magnet-) > 100 $\mu\text{g/mL}$ (Magnet+) > 100 $\mu\text{g/mL}$ (Magnet-) (Figure 9A). For the group of 100 $\mu\text{g/mL}$ (Magnet+), the temperature was raised to 47 °C after receiving 20 minutes of AMF application. Under such magnetic-induced hyperthermia circumstance, the viability of Tramp-C1 cells was measured using MTT assay (Figure 9B). Significant cancer cell viability decreased (~87.3%) was observed from cells received magnet-enhanced STM-SPIO internalization following by 20 minutes of AMF application. In addition, it was noticed that nearly 100% viability was observed from cells received STM-SPIO without AMF treatment indicating the negligible cytotoxicity of this biomimetic nanomaterials.

Conclusions

In this study, we reported the fabrication, characterizations and applications of a novel biomimetic STM-SPIO system. Water-soluble STM-SPIO was successfully prepared via a simple sonication method. Coating of STM to SPIO significantly decreased the macrophage uptake. Magnetic hyperthermia-mediated cell death was observed from cells internalized with STM-SPIO following by AMF exposure *in vitro*. These results demonstrate the great potential of STM-SPIO as a novel biomimetic nanoparticulate system for future theranostic applications.

Acknowledgements

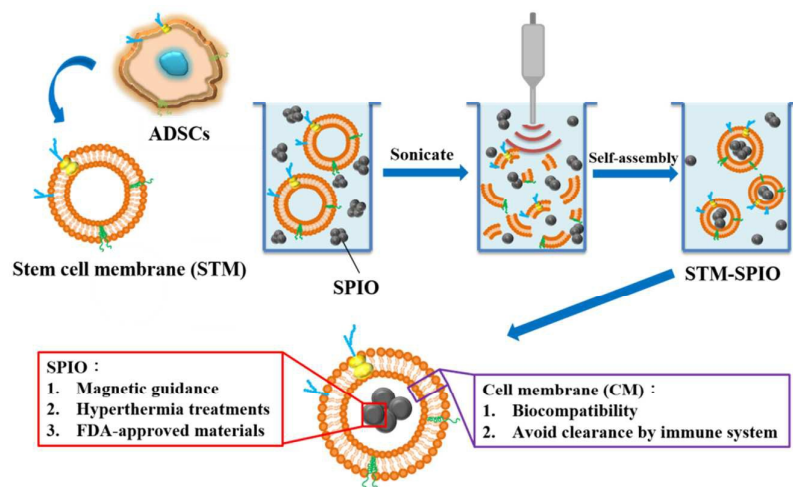
This research was financially supported by Ministry of Science and Technology of Taiwan (102-2113-M-007-006-MY2), National Health Research Institutes (NHRI) of Taiwan (NHRI-EX103-10221EC) and National Tsing Hua University (104N2046E1/104N2732E1). We thank to Ms. C.-Y. Chien of Ministry of Science and Technology (National Taiwan University) for the assistance in TEM experiments and to 7T animal MRI Core Lab of the Neurobiology and Cognitive Science Center, National Taiwan University for technical and facility supports. The magnetization was measured by using SQUID magnetometer (MPMS XL-7) at the National Chiao Tung University.

Notes and references

1. C. C. Chuang and C. W. Chang, *ACS applied materials & interfaces*, 2015, **7**, 7724-7731.
2. R. Y. Huang, P. H. Chiang, W. C. Hsiao, C. C. Chuang and C. W. Chang, *Langmuir*, 2015, **31**, 6523-6531.
3. C. Ayala-Orozco, C. Urban, M. W. Knight, A. S. Urban, O. Neumann, S. W. Bishnoi, S. Mukherjee, A. M. Goodman, H. Charron, T. Mitchell, M. Shea, R. Roy, S. Nanda, R. Schiff, N. J. Halas and A. Joshi, *ACS Nano*, 2014, **8**, 6372-6381.
4. G. Huang, G. Tong, J. Liu, L. Chen, W. Zhang, C. Quan, Q. Jiang, H. Sun and C. Zhang, *International Journal of Polymeric Materials*, 2015, **64**, 400-405.
5. J. Fang, H. Nakamura and H. Maeda, *Adv Drug Deliver Rev*, 2011, **63**, 136-151.
6. H. Otsuka, Y. Nagasaki and K. Kataoka, *Adv Drug Deliver Rev*, 2012, **64**, 246-255.
7. K. Knop, R. Hoogenboom, D. Fischer and U. S. Schubert, *Angewandte Chemie*, 2010, **49**, 6288-6308.

8. X. Wang, T. Ishida and H. Kiwada, *Journal of controlled release*, 2007, **119**, 236-244.
9. P. A. Oldenborg, A. Zheleznyak, Y. F. Fang, C. F. Lagenaur, H. D. Gresham and F. P. Lindberg, *Science*, 2000, **288**, 2051-2054.
10. C. C. Hsieh, S. T. Kang, Y. H. Lin, Y. J. Ho, C. H. Wang, C. K. Yeh and C. W. Chang, *Theranostics*, 2015, **5**, 1264-1274.
11. C. M. Hu, L. Zhang, S. Aryal, C. Cheung, R. H. Fang and L. Zhang, *Proceedings of the National Academy of Sciences of the United States of America*, 2011, **108**, 10980-10985.
12. A. Parodi, N. Quattrocchi, A. L. van de Ven, C. Chiappini, M. Evangelopoulos, J. O. Martinez, B. S. Brown, S. Z. Khaled, I. K. Yazdi, M. V. Enzo, L. Isenhardt, M. Ferrari and E. Tasciotti, *Nature Nanotechnology*, 2013, **8**, 61-68.
13. J. H. Fang, Y. T. Lee, W. H. Chiang and S. H. Hu, *Small*, 2015, DOI: 10.1002/smll.201402969.
14. M. Mahmoudi, S. Sant, B. Wang, S. Laurent and T. Sen, *Adv Drug Deliv Rev*, 2011, **63**, 24-46.
15. P. Bianco, X. Cao, P. S. Frenette, J. J. Mao, P. G. Robey, P. J. Simmons and C. Y. Wang, *Nature medicine*, 2013, **19**, 35-42.
16. M. P. De Miguel, S. Fuentes-Julian, A. Blazquez-Martinez, C. Y. Pascual, M. A. Aller, J. Arias and F. Arnalich-Montiel, *Current molecular medicine*, 2012, **12**, 574-591.
17. M. D. Swartzlander, A. K. Blakney, L. D. Amer, K. D. Hankenson, T. R. Kyriakides and S. J. Bryant, *Biomaterials*, 2015, **41**, 79-88.
18. M. Brahler, R. Georgieva, N. Buske, A. Muller, S. Muller, J. Pinkernelle, U. Teichgraber, A. Voigt and H. Baumler, *Nano letters*, 2006, **6**, 2505-2509.
19. A. K. Gupta and M. Gupta, *Biomaterials*, 2005, **26**, 1565-1573.
20. B. T. Estes, B. O. Diekman, J. M. Gimble and F. Guilak, *Nature protocols*, 2010, **5**, 1294-1311.
21. N. E. Toledano Furman, Y. Lupu-Haber, T. Bronshtein, L. Kaneti, N. Letko, E. Weinstein, L. Baruch and M. Machluf, *Nano letters*, 2013, **13**, 3248-3255.
22. E. A. Schultz-Sikma, H. M. Joshi, Q. Ma, K. W. Macrenaris, A. L. Eckermann, V. P. Dravid and T. J. Meade, *Chemistry of materials*, 2011, **23**, 2657-2664.
23. D. Eberbeck, M. Kettering, C. Bergemann, P. Zirpel, I. Hilger and L. Trahms, *J Phys D Appl Phys*, 2010, **43**.
24. Y. H. Bae and K. Park, *Journal of Controlled Release*, 2011, **153**, 198-205.
25. S. Huth, J. Lausier, S. W. Gersting, C. Rudolph, C. Plank, U. Welsch and J. Rosenecker, *J Gene Med*, 2004, **6**, 923-936.

Scheme



Scheme 1. Schematic representation of STM-SPIO preparation procedure.

Figures

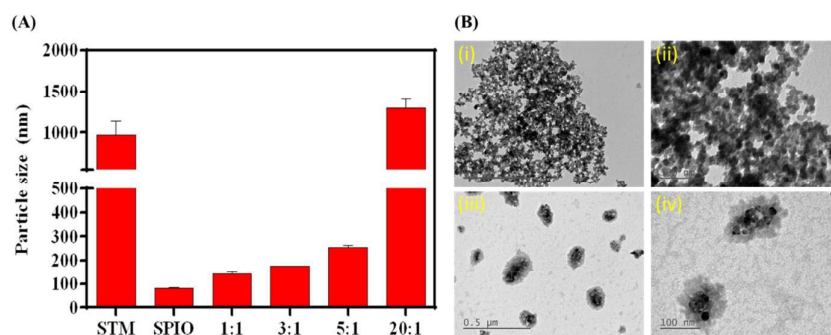


Figure 1. Characterizations of STM-SPIO (A) Effect of STM coating on the particle size of STM-SPIO. (B) TEM images of SPIO (i/ii) and STM-SPIO (iii/iv).

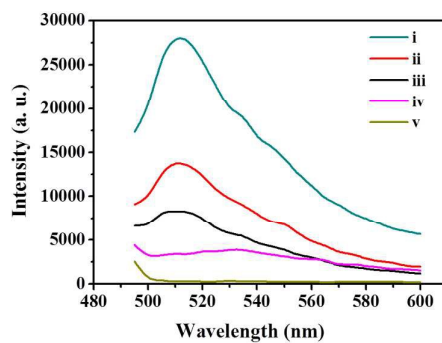


Figure 2. Verification of STM coating on SPIO using the dye retention assay. Fluorescence spectrum was taken (from top to down): (i) STM-SPIO + DiO (High). (ii) STM-SPIO + DiO (Low). (iii) Unmodified SPIO + DiO. (iv) STM. (v) Unmodified SPIO. (Ex: 460 nm / Em: 495-600 nm).

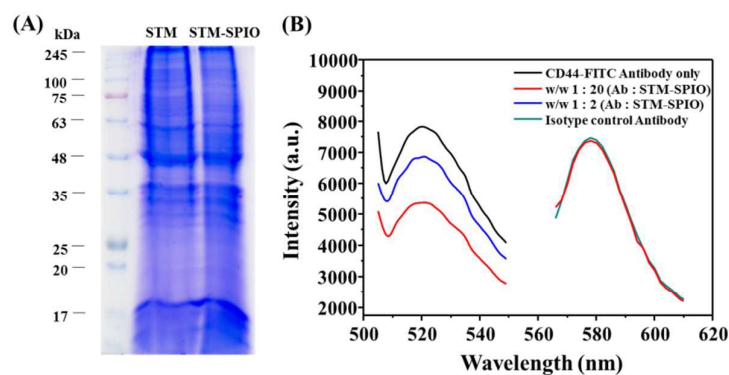


Figure 3. (A) Membrane protein retention analysis by SDS-PAGE. The total protein profile was comparable between STM and STM-SPIO. (B) Retention assay of stem cell-specific makers (CD44) on STM-SPIO. FITC-labelled anti-CD44 antibody (CD44-FITC) was incubated with STM-SPIO at w/w 1:20 or 1:2. A centrifuge step was performed to spin down STM-SPIO along with the bound CD44-FITC. The fluorescence spectrum of the free CD44-FITC in the supernatant fraction was analyzed. An isotype antibody was used as the negative control.

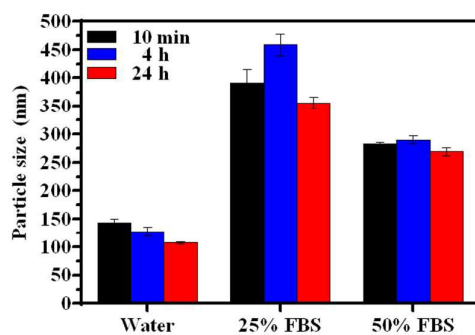


Figure 4. Colloidal stability of STM-SPIO in DI H₂O, 25% FBS/DMEM or 50% FBS/DMEM. The particle size was measured after incubating the nanoparticles in the designated environments for 10 minutes, 4 hours and 24 hours.

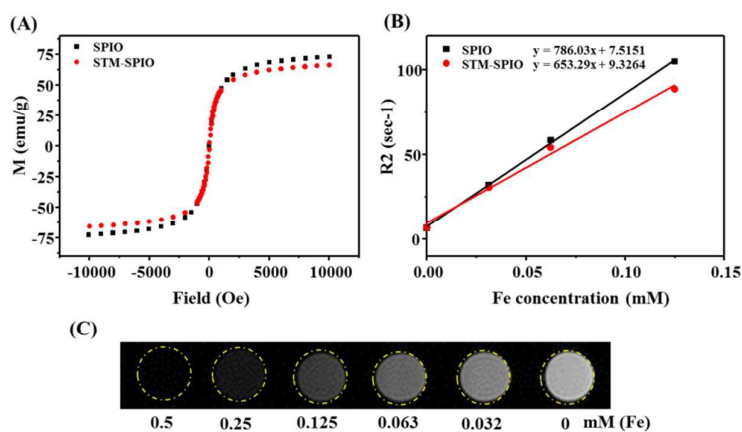


Figure 5. Magnetic properties and MR imaging of STM-SPIO. (A) Magnetism and hysteresis loop of and STM-SPIO measured by SQUID within 1 Tesla. (B) Transverse relaxivities (r_2) and (C) T2-weighted imaging of STM-SPIO at different concentration was measured by 7T MR imaging system (TR/TE = 6000 ms / 11 ms).

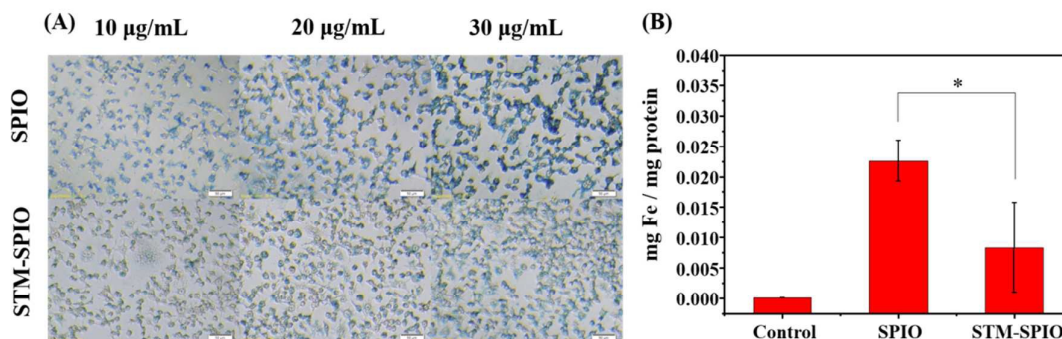


Figure 6. (A) Macrophages uptake of SPIO and STM-SPIO. Macrophages were incubated with various concentrations (10, 20 and 30 µg/mL) of SPIO (Top) or STM-SPIO (Bottom), then observed using Persian blue staining. (B) Quantitative measurement of intracellular Fe level in the macrophages by using ICP-MS. Data represents the mean \pm S.E.; n=3.

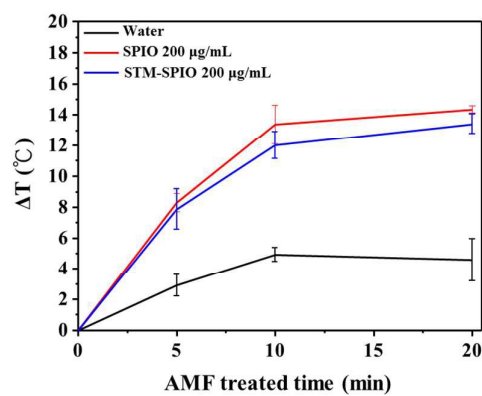


Figure 7. Magnetohyperthermia effect of STM-SPIO. The temperature of SPIO or STM-SPIO solution under AMF treatment for 20 minutes was recorded using an infrared thermal camera. Data represents the mean \pm S.E.; $n=3$.

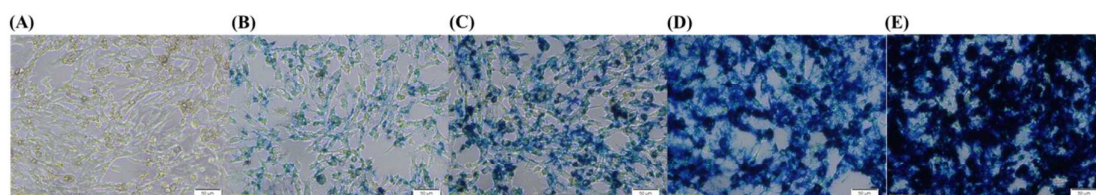


Figure 8. Magnetically-assisted cellular uptake of STM-SPIO by TRAMP-C1 cells. Cancer cells were incubated with (A) no treatment. (B) STM-SPIO (20 µg/mL) w/o magnet attraction. (C) STM-SPIO (20 µg/mL) w/ magnet attraction. (D) STM-SPIO (150 µg/mL) w/o magnet attraction. (E) STM-SPIO (150 µg/mL) w/ magnet attraction. Cellular uptake of SPIO was observed by Prussian Blue Staining.

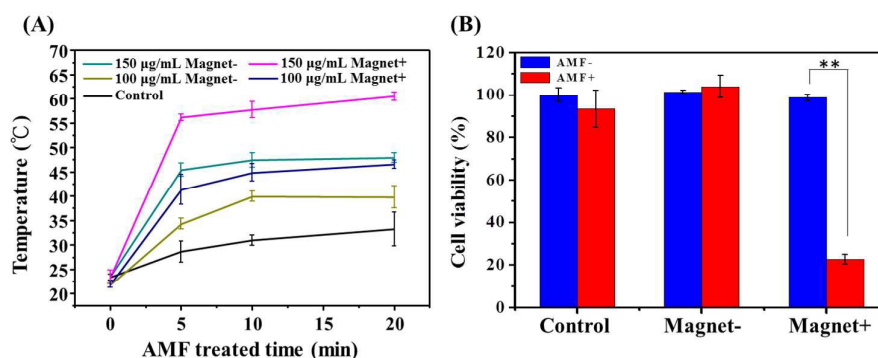


Figure 9. STM-SPIO-mediated magnetic hyperthermia treatment on TRAMP-C1 cells. (A) Effect of AMF treatment on the temperature of cell solutions. Green line: cells incubated with 100 µg/mL STM-SPIO without magnetic attraction (Magnet-). Blue line: cells incubated with 100 µg/mL STM-SPIO with magnetic attraction (Magnet+). Cyan line: cells incubated with 150 µg/mL STM-SPIO without magnetic attraction (Magnet-). Pink line: cells incubated with 150 µg/mL STM-SPIO with magnetic attraction (Magnet+). (B) Viability assay of TRAMP-C1 cells incubated with 100 µg/mL STM-SPIO with or without magnetic attraction then received AMF treatment. The cell viability was measured using MTT assay. Data represents the mean ± S.E.; n=3.

Biomimetic Stem Cell Membrane-Camouflaged Iron Oxide Nanoparticles for Theranostic Applications

Pei-Ying Lai[§], Rih-Yang Huang[§], Ssu-Yu Lin[§], Yee-Hsien Lin, Chien-Wen Chang*

Table of contents

In this study, for the first time, stem cell membrane (STM)-camouflaged superparamagnetic iron oxide nanoparticles (SPIO) were prepared and demonstrated for the potential theranostic applications.

